


 CrossMark
click for updates

 Cite this: *RSC Adv.*, 2014, 4, 38379

Fabrication of micro-optical elements on curved substrates by electrostatic induced lithography

 H. Li,^{ab} W. Yu,^{*a} T. Wang,^a H. Zhang,^a W. Niu,^a E. Abraham^c and M. P. Y. Desmulliez^{*c}

This article reports the fabrication and characterization of polymeric micro-optical elements on curved substrates using electrostatic induced lithography. Unlike previous studies focusing upon the pattern formation on planar substrates, we have extended this process by adding it to the micro-transfer molding process to obtain micro-optical elements like diffractive grating and microlenses on curved substrates with aspect ratio greater than 4 : 1. The optical test results of the fabricated micro-optical elements show a slight deviation from theoretical values due to the effect of the curved surface. In comparison with previous reported methods, *e.g.* laser direct writing or the capillary force lithography method, the method proposed here is faster and more flexible. More importantly, microstructures with high aspect ratio can be easily obtained, which is normally difficult for the two methods reported previously. Therefore, this technology can be used as an effective method for the fabrication of such components with microscale or even nanoscale feature size on curved surfaces.

 Received 17th June 2014
Accepted 11th August 2014

DOI: 10.1039/c4ra05823b

www.rsc.org/advances

Introduction

Applications of micro- and nano-patterned surfaces are widespread in microelectronics, photonics, information storage devices, MEMS/NEMS, sensors and biomedical devices. Recently, patterning technologies have been applied to curved surfaces with resolution down to the submicron scale. The methods researched were laser direct writing lithography,^{1,2} capillary force lithography,³ step-and-flash lithography⁴ and others.^{5–8} The laser direct writing method uses the focused beam spot to define the patterns point by point, which is hence very inefficient. For capillary force lithography, the pattern is formed by driving the fluidic polymer into the capillary cavity under elevated temperature. Therefore, it is also time consuming because normally long thermal cycle needs to be conducted during the process. In addition, it is difficult to achieve microstructures with very high aspect ratio.³ Step and flash imprinting method and soft lithography method all suffer from the difficulty to separate the mould from substrate due to their close contact during the manufacturing process.

EIL has attracted a lot of attention over the last ten years as this technology combines top-down and bottom-up approaches and is able to achieve polymeric micro/nanostructures in a

single process step. In addition, EIL does not require expensive equipment and photosensitive materials in comparison with traditional photolithography methods. More importantly, EIL is a noncontact lithographic method, which does not suffer from the contamination problem of the master mould. The underlying physical phenomenon responsible for this technique, the instability of polymer films on planar substrates when exposed to an external electric field, has also been intensively researched from the theoretical and experimental points of view, and structures including columns, ridges, holes, channels and even hollow structures have been demonstrated.^{9–22} However, the stability of a thin film on a curved surface is rather different from the planar one. For the case of the flat surface, the electric field overcomes the in-plane curvature to engender structures like columns, holes, or channels on the film. However, for the case of the curved surface, the radial curvature force plays a role in the destabilization of the film as well. Recently, theoretical studies about the pattern formation on curved surfaces induced by electrostatic field were conducted by V. Anoop Kishore²³ and Bo Li.²⁴ In these studies, the dimension of the radius of curvature was in the micrometer scale and thus the resulting radial curvature force had a great impact on the film destabilization. It was demonstrated that the electric field must be strong enough to overwhelm this force so that ridge structures can be formed on the curved surface. Experimental work about the formation of three-dimensional microstructures on such curved surfaces was not greatly reported. In contrast we mainly study the pattern formation on curved surfaces with millimeter scale radius of curvature. The influence of the radial curvature force is relatively small so that it is easier to control the customized pattern formation process by simply controlling the intensity of

^aState Key Laboratory of Applied Optics, Changchun Institute of Optics, Fine Mechanics & Physics, Chinese Academy of Sciences, No. 3888, Dongnanhu Road, Changchun, Jilin, P.R.China. E-mail: yuwx@ciomp.ac.cn; Fax: +86 0431 86176058; Tel: +86 0431 86176058

^bUniversity of Chinese Academy of Sciences, Beijing, 100049, P.R. China

^cMicroSystems Engineering Centre (MISEC), School of Engineering & Physical Sciences, Heriot-Watt University, Edinburgh EH14 4AS, UK. E-mail: m.desmulliez@hw.ac.uk; Fax: +44 (0)131 451 4155; Tel: +44 (0)131 451 3340

the applied electric field. Specifically, we demonstrate the successful fabrication of micro-optical elements on curved surfaces with 40 mm radius of curvature by combining micro-transfer molding²⁵ and electro-hydrodynamic instability patterning.²⁶ In particular we demonstrate the manufacturing of microstructures on concave and convex surfaces. Grating microstructures of 8.75 μm width and 36 μm height patterned on a concave surface have been obtained and characterized. The high aspect ratio (4 : 1) concave grating has good self-focusing and dispersion properties. Such structures could prove useful in optical encoding where gratings are often placed on rotating pieces of machinery. These preliminary results show the great potential of the EIL method for the fabrication of micro- and nanostructures on curved surfaces. In addition, microlens array with each lens has a diameter of 4 μm and a period of 10 μm has also been fabricated on a concave surface successfully. This demonstrates the flexibility of the method on the fabrication of various micro-optical elements for different application purposes.

Materials and method

The schematic of the combined process applied for the fabrication of Diffractive Optical Elements (DOEs) on a curved surface is presented in Fig. 1. The whole process has five main steps: (1) fabrication of DOEs on a planar substrate by a traditional photolithographic process; (2) fabrication of reversed DOEs in PDMS using soft lithography; (3) fabrication of DOEs on a convex surface *via* the micro-transfer molding method; (4) deposition of a 200 nm thick Cr layer onto the DOEs by electron-beam evaporation to serve as the conductive master electrode in the EIL process; (5) fabrication of DOEs in SU8 polymer *via* the EIL method. The PDMS is prepared by mixing the prepolymer with crosslink agent (10 : 1 wt ratio) and cured for 24 h at room temperature.

The EIL experimental setup for the micro-fabrication of DOEs on 3D surfaces is illustrated in Fig. 2, where two conformal cylindrical convex/concave surfaces, separated by a uniform air gap of 60 μm thanks to dielectric spacers, are used

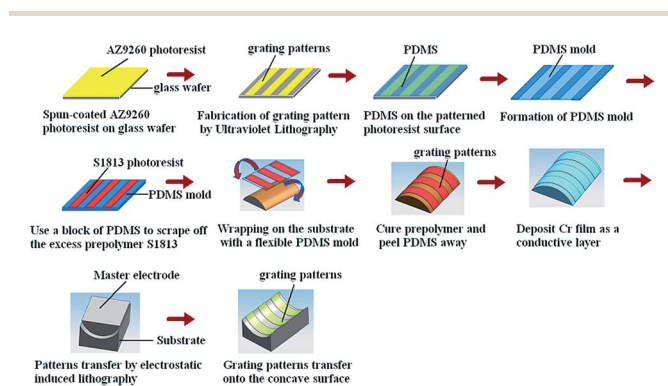


Fig. 1 Schematic of the combined micro-transfer molding and electrostatic induced lithography process: preparation of the gratings onto a planar surface (first five steps), gratings transfer on the convex surface (steps six and seven) and manufacturing of the patterns onto the concave surface by the EIL method (last three steps).

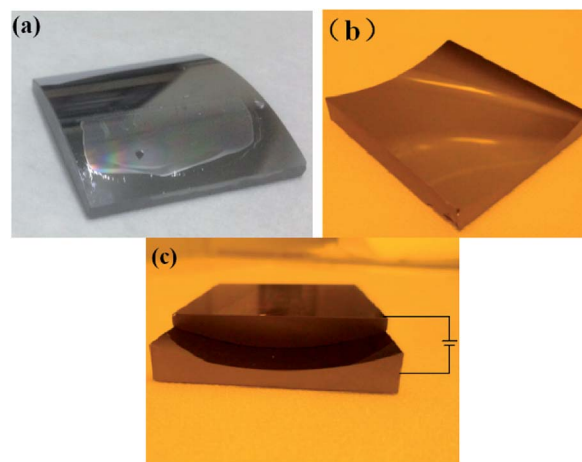


Fig. 2 Experimental setup used for the micro-fabrication of DOEs on concave surfaces. (a) The grating microstructure has been transferred previously onto the convex surface of a planar-convex cylinder lens by the micro-transfer molding method; (b) a planar-concave cylinder lens is used as the substrate onto which a positive image of the master electrode will be grown through the EIL method; (c) the experimental setup for the EIL process with the master electrode at the top.

as curved electrodes. The radius of curvature of the mask and the convex substrate is 46.512 mm and 46.572 mm, respectively. The convex surface of the top electrode, shown in Fig. 2(a), has been patterned with microscale gratings by the micro-transfer molding method. A thin layer of Cr was deposited on the top of the microstructures to make them electrically conductive. Fig. 3 shows the top view image and 3-D profile of the gratings obtained in Fig. 2(a). The SU8 polymer film is coated onto the concave cylindrical surface by the dip coating method.²⁷ SU8-5 is selected as the polymeric material due to its relatively low viscosity and short curing time. The whole electrostatic induced patterning process lasts about fifteen minutes during which the experimental setup is kept at 135 $^{\circ}\text{C}$ and then allowed to cool at room temperature. During that time, a DC voltage of 102 V is applied between the two electrodes, as shown in Fig. 2(c). The DC voltage is switched off only after the temperature drops down to room temperature and the electrostatic induced microstructure is solidified. After the cooling-down phase, the planar-concave cylindrical lens is separated gently to avoid the breakage of the formed structure. Further details on a similar

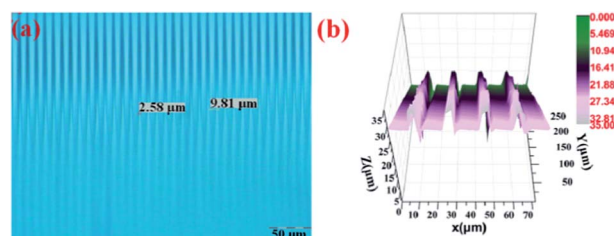


Fig. 3 (a) Optical microscope image of the fabricated grating structure on a convex curved surface by micro-transfer molding (top view). (b) 3D surface profile of the fabricated structure measured by laser scanning confocal microscopy.

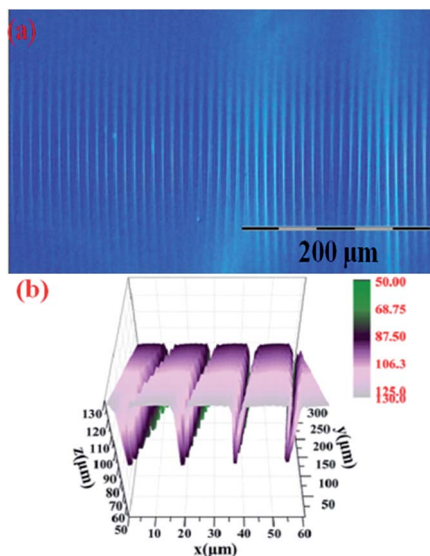


Fig. 4 (a) Optical micrograph of the fabricated grating on a concave curved surface by the EIL method; (b) 3D surface profile of the fabricated structure measured by laser scanning confocal microscopy. A 34 μm thick SU8 polymer film was annealed for 15 minutes at 135 $^{\circ}\text{C}$ with an applied voltage $U = 102$ V.

process applied to planar surfaces can be obtained in ref. 26 and 28. The same technique can be applied to planar-convex lenses.

Fabrication results and discussions

Fig. 3 shows the grating formed by micro-transfer molding on the convex surface of the cylinder. The image of the grating obtained by optical microscopy in Fig. 3(a) becomes blurred on the edge due to the curved surface. Fig. 3(b) provides the 3D surface profile of the grating measured by laser scanning confocal microscopy (BX61, Olympus). The grating has a period of 9.81 μm , a width of 2.58 μm and a height of around 5 μm , giving therefore an aspect ratio of around 2 : 1.

The convex cylindrical surface patterned with the grating structure is then used as the master electrode after deposition

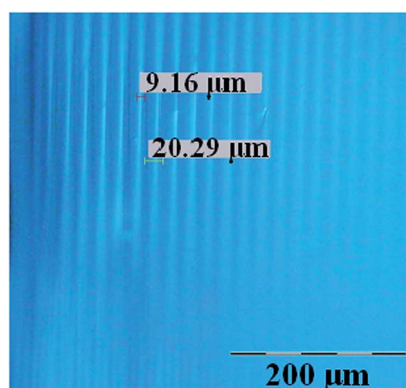


Fig. 5 Grating microstructures with a width of about 9.16 μm and a period of 20.29 μm . A 22 μm thick SU8 polymer film was annealed for 12 minutes at 135 $^{\circ}\text{C}$ with an applied voltage of 125 V.

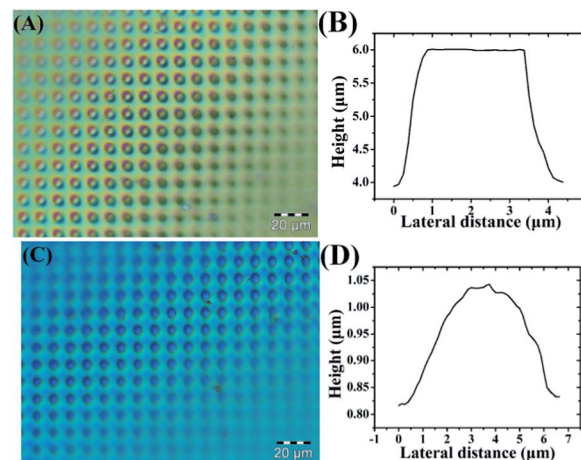


Fig. 6 Optical micrographs and 2D surface profiles of the fabricated microcylinder on the curved surface. (a) Microcylinder fabricated by micro-transfer molding; (b) 2D surface profile of the fabricated microcylinder of (a) measured by laser scanning confocal microscopy; (c) microlens obtained by the EIL method; (d) 2D surface profile of the fabricated microlens of (c) measured by laser scanning confocal microscopy.

of a 200 nm thick Cr layer. Fig. 4 shows the microstructures fabricated in polymer on the concave surface by the EIL method. The initial film thickness was 34 μm , the annealing time is 15 minutes and the applied voltage is 102 V. As shown in Fig. 4, the fabricated grating microstructure has a width of 8.75 μm and a height of 36 μm , giving an aspect ratio of higher than 4 : 1. Although the pattern on the master electrode has only an aspect ratio of about 2 : 1, by controlling the appropriate process parameters, microstructures with higher aspect ratio higher than the master electrode can be obtained. The fabricated grating microstructure has the same period as that of the grating on the master but the filling ratio is different. For the master grating, the filling ratio is about 25.8%, compared to 87.5% for the fabricated grating. Again, such a ratio can be controlled by carefully tuning the process parameters, which include the initial film thickness, the distance between two electrodes, the applied voltage, *etc.*

When the two electrode surfaces are not perfectly parallel, the electric field distribution varies slightly across the substrate

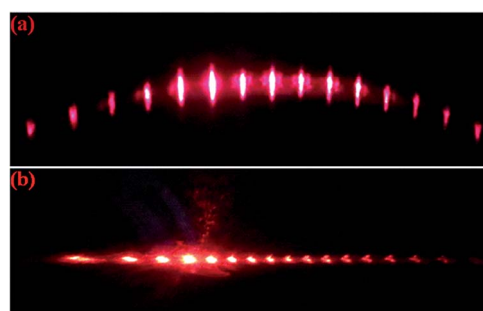


Fig. 7 Diffraction patterns of the fabricated grating with period about 10 μm on (a) the convex surface shown in Fig. 3 and (b) the concave surface shown in Fig. 4.

Table 1 Measured diffraction efficiency of the fabricated microstructures with 10 μm period

Diffraction order	-3	-2	-1	0	1	2	3
Measured diffraction efficiency (Fig. 7(b))	0.0046	0.0143	0.0392	0.0714	0.0371	0.0164	0.0093
Calculated diffraction efficiency (Fig. 7(b))	0.0014	0.0029	0.0057	0.0511	0.0057	0.0029	0.0014

surface such that a grating with gradual changing profile is obtained. On the left side of the Fig. 5 and using another master electrode with larger feature sizes, grating microstructures with width of 9.16 μm and period of 20.29 μm can be clearly seen. However, the polymer film on the right side of the picture does not have the clearly defined grating microstructures seen on the left of the image. The plausible reason for this imperfection is that the air gap between two electrodes is not uniform so that the electrostatic field is not strong enough to destabilize the film in order to form the desired microstructure.

In addition, the fabrication of microlens on a curved surface is demonstrated as well. Fig. 6(a) and (b) show the microcylinder array fabricated by micro-transfer molding on the convex surface. The microcylinder has a period of 10 μm , a diameter of about 4 μm and a height of around 2 μm . Fig. 6(c) and (d) show the microlens array fabricated in polymer on the concave surface by the EIL method by using the mask electrode shown in Fig. 6(a) and (b). The initial polymeric film has a thickness of 35.15 μm , the annealing time is 10 minutes and the applied voltage is 400 V. As shown in Fig. 6(c) and (d), the fabricated microlens has a diameter of 6 μm and a height of 225 nm. It should be noted that though the surface profile of the microstructures on the master electrode has a binary shape, microlens with a continuous surface profile can still be fabricated on the curved surface. This is a great advantage for the combining method demonstrated in this work in that a master patterned with microstructures with continuous surface profile is rather difficult to be fabricated. By using a binary master instead, one can save the time and cost for the fabrication of 3-D microstructures significantly.

Optical test results and discussion

To characterize the optical properties of the fabricated grating obtained on the convex surface (Fig. 3) and the concave surface (Fig. 4), a He-Ne laser with 1.5 mm beam diameter is used to illuminate the microstructures to generate the diffractive patterns as shown in Fig. 7. As shown in Fig. 7(a), the 10 μm period grating displays more than ten diffraction orders. The asymmetric distribution of the pattern is the result of the oblique incidence of the laser beam. The diffractive efficiency of the first seven orders has been measured by a power meter with a resolution of 0.01 μW and an effective detecting area of more than 100 mm^2 . The detecting area of the power meter is large enough to cover the diffracted spots although the beam spot of some higher orders is not well focused into a small spot. To the best of the authors' knowledge, a theoretical model does not exist for the calculation of the diffraction efficiency of a grating obtained on a curved surface. Using rigorous coupled wave analysis, the diffraction efficiency model for a planar grating of

similar period and step height was therefore used. The calculated and measured diffraction efficiency results of the first seven diffraction orders are listed in Table 1. A slight deviation between the theoretical and experimental results is witnessed, which might be due to the appropriateness of the model. In order to accurately simulate the diffractive grating on 3-D curved substrates, a new model would need to be developed.

Conclusions

We have successfully demonstrated the feasibility of patterning diffractive optical elements at micrometer scale on concave surfaces using the EIL method. The resulting DOE was also characterized and fair agreement between the theoretical calculations and experimental results of the diffraction efficiency of the grating was obtained. The preliminary results indicate that this method has great potential for the micro and even nanofabrication on 3D curved surfaces such as those required for optical encoding.^{28,29} In comparison with methods reported previously, EIL method provides a rather simple, flexible and yet cost-effective route for the micro-fabrication of microstructures with a high aspect ratio. More importantly, it is a noncontact lithographic method and does not suffer from the mould contamination problem, which allows the reuse of the mould and therefore saves process costs further. We believe it can be applied for the fabrication of microstructures on 3D curved surfaces for applications including microelectronics, photonics and MEMS.

Acknowledgements

The authors acknowledge the financial support from Natural Science Foundation of China under grant numbers 61361166004, 90923036 and 60977041 as well as the Ministry of Sciences and Technology of China under grant number 2010DFR10660. The financial support of the UK Innovative electronic Manufacturing Research Centre (IeMRC) is also acknowledged through the funding of the Flagship project "Smart Microsystems" (FS/01/02/10).

Notes and references

- 1 Y. Xie, Z. Lu and F. Li, *Opt. Express*, 2003, **11**, 992–995.
- 2 T. Wang, W. Yu, D. Zhang, C. Li, H. Zhang, W. Xu, Z. Xu, H. Liu, Q. Sun and Z. Lu, *Optics Express*, 2010, **18**, 25102–25107.
- 3 D. Zhang, W. Yu, T. Wang, Z. Lu and Q. Sun, *Opt. Express*, 2010, **18**, 15009–15016.
- 4 P. Ruchhoeft, M. Colburn, B. Choi, H. Nounu, S. Johnson, T. Bailey, S. Damle, M. Stewart, J. Ekerdt, S. V. Sreenivasan,

- J. C. Wolfe and C. G. Willson, *J. Vac. Sci. Technol., B: Microelectron. Nanometer Struct.–Process., Meas., Phenom.*, 1999, **17**, 2965–2969.
- 5 W. Mook Choi and O. Ok Park, *Nanotechnology*, 2004, **15**, 1767–1770.
- 6 L. Li and A. Y. Yi, *J. Micromech. Microeng.*, 2009, **19**, 105010.
- 7 M. N. De Silva, J. Paulsen, M. J. Renn and D. J. Odde, *Biotechnol. Bioeng.*, 2006, **93**, 919–927.
- 8 T. Wang, W. Yu, D. Zhang, C. Li, H. Zhang, W. Xu, Z. Xu, H. Liu, Q. Sun and Z. Lu, *Opt. Express*, 2010, **18**, 25102–25107.
- 9 Z. Lin, T. Kerle, S. M. Baker and D. A. Hoagland, *J. Chem. Phys.*, 2001, **114**, 2377–2381.
- 10 E. Schaffer, T. Thurn-Albrecht, T. P. Russell and U. Steiner, *Europhys. Lett.*, 2001, **53**, 518–524.
- 11 R. Verma, A. Sharma, K. Kargupta and J. Bhaumik, *Langmuir*, 2005, **21**, 3710–3721.
- 12 Z. Lin, T. Kerle and T. P. Russell, *Macromolecules*, 2002, **35**, 3971–3976.
- 13 J. Sarkar and A. Sharma, *Phys. Rev. E: Stat., Nonlinear, Soft Matter Phys.*, 2008, **77**, 031604.
- 14 T. Y. Hin, C. Liu, P. P. Conway, W. Yu and M. P. Y. Desmulliez, *IEEE Photonics Technol. Lett.*, 2010, **22**, 957–959.
- 15 X. Lei, L. Wu, P. Deshpande, Z. Yu, W. Wu, H. Ge and S. Y. Chou, *Nanotechnology*, 2003, **14**, 786–790.
- 16 P. Deshpande, X. Sun and S. Y. Chou, *Appl. Phys. Lett.*, 2001, **79**, 1688–1690.
- 17 L. Wu and S. Y. Chou, *Appl. Phys. Lett.*, 2003, **82**, 3200–3202.
- 18 N. E. Voicu, S. Harkema and U. Steiner, *Adv. Funct. Mater.*, 2006, **16**, 926–934.
- 19 N. E. Voicu, M. S. M. Saifullah, K. R. V. Subramanian, M. E. Welland and U. Steiner, *Soft Matter*, 2007, **3**, 554–557.
- 20 J. Heier, J. Groenewold and U. Steiner, *Soft Matter*, 2009, **5**, 3997–4005.
- 21 X. Li, J. Shao, Y. Ding, H. Tian and H. Liu, *J. Micromech. Microeng.*, 2011, **21**, 115004.
- 22 H. Chen, W. Yu, S. Cargill, M. K. Patel, C. Bailey, C. Tonry and M. P. Y. Desmulliez, *Microfluid. Nanofluid.*, 2012, **13**, 75–82.
- 23 V. Anoop Kishore and D. Bandyopadhyay, *J. Phys. Chem. C*, 2012, **116**, 6215–6221.
- 24 B. Li, Y. Li, G.-K. Xu and Xi.-Q. Feng, *J. Phys.: Condens. Matter*, 2009, **21**, 445006.
- 25 X.-M. Zhao, Y. Xia and G. M. Whitesides, *Adv. Mater.*, 1996, **8**, 837–840.
- 26 G. Liu, W. Yu, H. Li, J. Gao, D. Flynn, R. W. Kay, S. Cargill, C. Tonry, M. K. Patel, C. Bailey and M. P. Y. Desmulliez, *J. Micromech. Microeng.*, 2013, **23**, 035018.
- 27 M. E. Spotnitz, D. Ryan and H. A. Stone, *J. Mater. Chem.*, 2004, **14**, 1299–1302.
- 28 H. Li, W. Yu, L. Zhang, Z. Liu, K. E. Brown, E. Abraham, S. Cargill, C. Tonry, M. K. Patel, C. Bailey and M. P. Y. Desmulliez, *RSC Adv.*, 2013, **3**, 11839–11845.
- 29 H. Li, W. Yu, Y. Wang, H. Bu, Z. Liu, E. Abraham and M. P. Y. Desmulliez, *RSC Adv.*, 2014, **4**, 13774.